High-turnover hypoiodite catalysis for asymmetric synthesis of tocopherols

Muhammet Uyanik *et al.*

Science **345**, 291 (2014);
DOI: 10.1126/science.1254976

Science (print ISSN 0036-8075; online ISSN 1095-9203) is published weekly, except the last week in December, by the American Association for the Advancement of Science, 1200 New York Avenue NW, Washington, DC 20005.

22. J. A. D. Matthew, M. Komninos, *Surf. Sci.* **53**, 716–725 (1975).
23. F. Tarantelli, L. S. Cederbaum, *Phys. Rev. Lett.* **71**, 649–652 (1993).
24. T. D. Thomas *et al.*, *Phys. Rev. Lett.* **89**, 223001 (2002).
25. A. Niehaus, *J. Phys. At. Mol. Opt. Phys.* **19**, 2925–2937 (1986).
26. V. May, O. Kühn, *Charge and Energy Transfer Dynamics in Molecular Systems*, (Wiley-VCH, Weinheim, 2011).
27. E. Hamilton *et al.*, *Phys. Rev. A* **72**, 043402 (2005).
28. V. Averbukh, L. S. Cederbaum, *J. Chem. Phys.* **123**, 204107 (2005).
29. M. Krikunova *et al.*, *New J. Phys.* **11**, 123019 (2009).

ACKNOWLEDGMENTS

Parts of this research were carried out at the Linac Coherent Light Source (LCLS) at the SLAC National Accelerator Laboratory. LCLS is an Office of Science User Facility operated for the U.S. Department of Energy Office of Science by Stanford University. We acknowledge the Max Planck Society for funding the development and operation of the CFEL-ASG-Multi-Purpose (CAMP) instrument within the Advanced Study Group at CFEL. A.R. acknowledges the support from Chemical Sciences, Geosciences, and Biosciences Division, Office of Basic Energy Sciences, Office of Science, U.S. Department of Energy and from Kansas National Science Foundation Experimental Program to Stimulate Competitive Research (NSF EPSCoR) "First Award"; D.R. acknowledges support from the Helmholtz Gemeinschaft through the Young Investigator Program. J. K and S. T. acknowledge support from the excellence cluster "The Hamburg Centre for Ultrafast Imaging - Structure, Dynamics and Control of Matter at the Atomic Scale" of the Deutsche Forschungsgemeinschaft. We are grateful to C. Schmidt for technical support, to M. Cryle for help with sample selection, and to the SLAC staff for their support and hospitality during the beamtime. We thank R. Moshammer, K. Schnorr A. Senftleben, and T. Pfeifer for fruitful discussions and for the idea to adapt the classical over-the-barrier model for the interpretation of the data presented in this manuscript.

SUPPLEMENTARY MATERIALS

www.sciencemag.org/content/345/6194/288/suppl/DC1
Materials and Methods
Figs. S1 to S4
Tables S1 to S3
References (*30*–*39*)

19 March 2014; accepted 9 June 2014
10.1126/science.1253607

ASYMMETRIC CATALYSIS

High-turnover hypoiodite catalysis for asymmetric synthesis of tocopherols

Muhammet Uyanik,[1] Hiroki Hayashi,[1] Kazuaki Ishihara[1,2]*

The diverse biological activities of tocopherols and their analogs have inspired considerable interest in the development of routes for their efficient asymmetric synthesis. Here, we report that chiral ammonium hypoiodite salts catalyze highly chemo- and enantioselective oxidative cyclization of γ-(2-hydroxyphenyl)ketones to 2-acyl chromans bearing a quaternary stereocenter, which serve as productive synthetic intermediates for tocopherols. Raman spectroscopic analysis of a solution of tetrabutylammonium iodide and *tert*-butyl hydroperoxide revealed the in situ generation of the hypoiodite salt as an unstable catalytic active species and triiodide salt as a stable inert species. A high-performance catalytic oxidation system (turnover number of ~200) has been achieved through reversible equilibration between hypoiodite and triiodide in the presence of potassium carbonate base. We anticipate that these findings will open further prospects for the development of high-turnover redox organocatalysis.

Biologically active compounds containing a chiral chroman skeleton are abundant in nature (*1*). One of the most prominent chiral chromans is α-tocopherol, which is in the same family as vitamin E, together with β-, γ-, and δ-tocopherols and the corresponding α-, β-, γ-, and δ-tocotrienols (Fig. 1A) (*2*). α-Tocopherol acts as a lipid-soluble, chain-breaking antioxidant by capturing free radicals or singlet oxygen formed by oxidative metabolism in tissues (*3*). Furthermore, tocopherols show physiologically diverse properties, including anti-tumor, anti-inflammatory, anti-atherosclerosis, and cell-signaling activities (*4*–*8*). Various non-natural tocopherol analogs have also been developed because of their potency and distinct structural features. For example, trolox and its derivatives have been used as a chiral derivatizing reagent (*9*) and NO-releasing drug candidates (*10*). Dihydrodaedalin A, a synthetic intermediate for the natural product daedalin A (*11*), is a potent tyrosinase inhibitor and has been shown to suppress melanogenesis in human skin without affecting cell viability (*12*). C48 developed by Merck research laboratories (Rahway, New Jersey) is a potent, selective peroxisome proliferator–activated receptor–α/γ dual agonist and exhibits substantial antihyperglycemic and hypolipidemic activities (*13*).

Natural *D*-α-tocopherol is formally (2*R*,4′*R*,8′*R*)-2,5,7,8-tetramethyl-2-(4′,8′,12′-trimethyltridecyl)-6-chromanol. The (2*R*)-configuration at the chroman ring among the three stereocenters of α-tocopherol is critical for its bioactivity; (2*S*)-stereoisomers are not accepted by the tocopherol transfer protein (*5*). Thus, asymmetric construction of the chroman ring has been an important challenge (*1*, *2*). Enantioselective processes have been developed to address this need by using chiral transition metal complexes (Pd or Ru) (*14*–*16*) or organocatalysts (*17*, *18*). However, the low catalytic activities and/or moderate enantioselectivities have limited their utility (*2*). Here, we report a transition metal–free (*19*) approach for the enantioselective synthesis of tocopherols and their analogs by using chiral hypoiodite catalysts (*20*, *21*) generated in situ from the corresponding quaternary ammonium iodide with alkyl hydroperoxides as environmentally benign co-oxidants (Fig. 1B). Chemoselective oxidative cyclization of hydroquinone-derived γ-(2-hydroxyphenyl)ketones

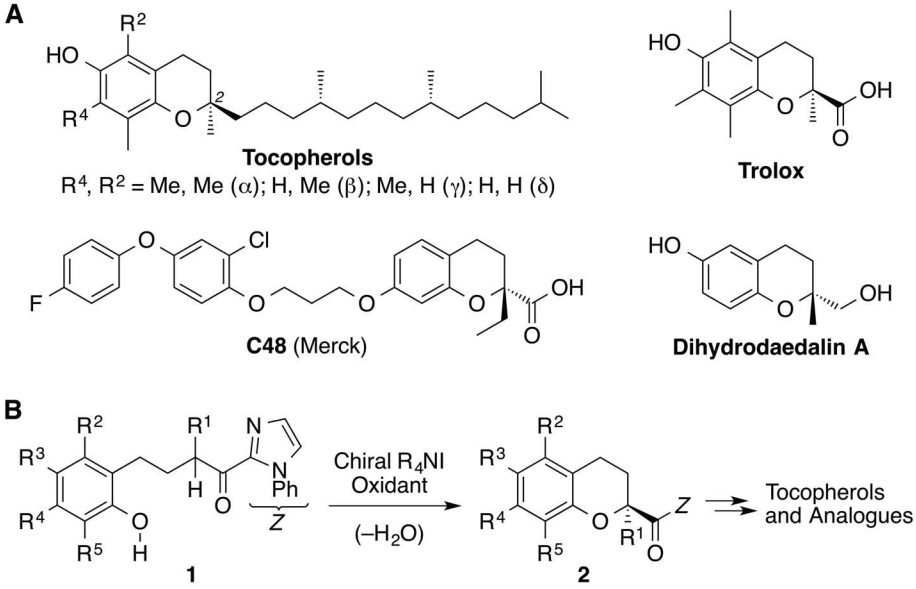

Fig. 1. A catalytic route to the tocopherol core. (**A**) Biologically active tocopherols and other chromans. (**B**) Enantioselective oxidative cycloetherification of γ-(2-hydroxyphenyl)ketones **1** to 2-acyl chromans **2** by in situ–generated chiral hypoiodite catalysts.

[1]Graduate School of Engineering, Nagoya University, Furo-cho, Chikusa, Nagoya 464-8603, Japan. [2]Core Research for Evolutional Science and Technology, Japan Science and Technology Agency, Furo-cho, Chikusa, Nagoya 464-8603, Japan.
***Corresponding author. E-mail: ishihara@cc.nagoya-u.ac.jp**

gives >95% yield of the corresponding 2-acyl chromans; with the quaternary stereocenter set in high enantioselectivity, these products are poised for elaboration to a range of tocopherols.

Previously, we developed in situ–generated chiral quaternary ammonium hypoiodite (R_4NOI) catalysis for the enantioselective oxidative cyclization of β-(2-hydroxyphenyl)ketones to the five-membered ring products 2-acyl-2,3-dihydrobenzofurans with hydrogen peroxide or *tert*-butyl hydroperoxide (TBHP) as co-oxidants (*20*). The use of chiral binaphthyl-based quaternary ammonium (*22*) iodide as a precatalyst and an *N*-phenylimidazol-2-yl (*Z*) (*23*) group as an auxiliary of β-(2-hydroxyphenyl) ketones was effective for inducing high enantioselectivities. We envisioned that the enantioselective oxidative cyclization of γ-(2-hydroxyphenyl) ketones (**1**) would give the desired six-membered ring 2-acyl chromans (**2**) (Fig. 1B).

To begin our investigation, we compared the enantioselective oxidative cyclization of (*5-tert*-butyldimethylsilyloxy-2-hydroxyphenyl)ketones (**1a** and ***3a***) derived from trimethyl hydroquinone (Fig. 2A). Oxidative cyclization of ***3a*** under previous conditions by using 10 mole percent (mol %) of ammonium iodide (*R*,*R*)-**5a** and hydrogen peroxide (2 equivalents) as an oxidant in methyl *tert*-butyl ether (MTBE) gave five-membered ring dihydrobenzofuran (*R*)-**4a** in 95% yield with 93% enantiomeric excess (ee). In sharp contrast, oxidative cyclization of **1a** to the six-membered ring under the same conditions was sluggish, and only a trace amount of the desired 2-acyl chroman **2a** was obtained together with a small amount (10% yield) of phenol-oxidation product **6a**.

The posited catalytic mechanism and side-reaction pathway are summarized in Fig. 2B. The above results and competition experiments (table S1) suggested that oxidative cyclization to a six-membered ring was much slower than cyclization to a five-membered ring. Thus, undesired side reactions, such as the dearomatization of **1a**, preferentially proceeded to give side-products **6a** and/or **6b**, presumably via phenoxenium ion **7** (*24*). The cyclization step might be rate-limiting for six-membered ring oxidative cyclization. Consequently, the in situ–generated catalytic active species (hypoiodite) was easily converted to an inert species such as triiodide salts, as confirmed with Raman analysis. For the construction of an efficient catalytic cycle, the oxidative cyclization step should not be rate-limiting. To address this issue, the oxidation of iodide (path **a**) should be decelerated, oxidative cyclization (path **b**) should be accelerated, or the inactivation (path **c**) should be suppressed or reversed. The use of TBHP as a weaker oxidant (*25*) instead of hydrogen peroxide solved this problem partially by deceleration of the generation of active species. Substrate **1a** was consumed within 1 hour; however, the desired product **2a** was obtained in only 15% yield with 18% ee (Fig. 2A). Undesired dearomatization dominated again, and quinone **6a** and peroxy quinol **6b** were obtained in a combined yield of 65%.

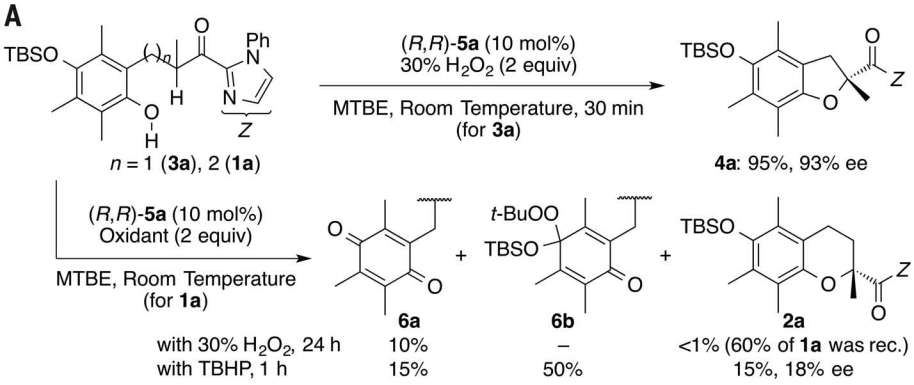

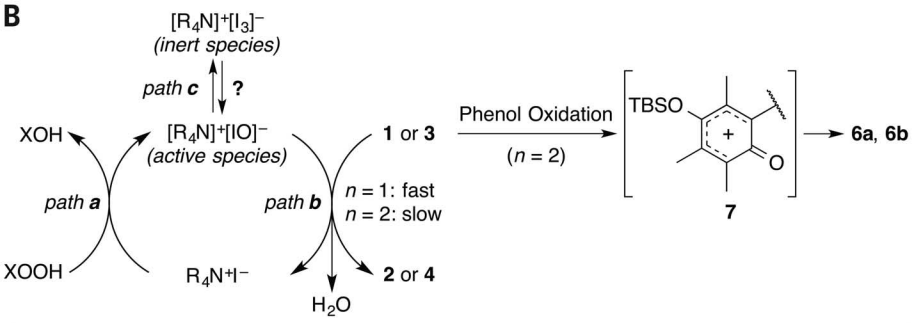

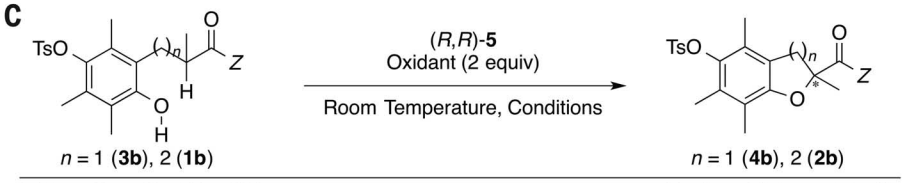

Entry	1b *or* 3b	5 (mol%)	Oxidant	Conditions	Product: Yield, ee (%, %)
1	**1b**	**5a** (10)	TBHP	MTBE, 3 h	(*R*)-**2b**: 98, 60
2	**1b**	**5b** (10)	TBHP	MTBE, 24 h	(*S*)-**2b**: 99, 86
3	**1b**	**5c** (10)	TBHP	MTBE, 24 h	(*S*)-**2b**: 94, 82
4	**1b**	**5d** (10)	TBHP	MTBE, 5 h	(*S*)-**2b**: 96, 89
5	**1b**	**5d** (10)	30% H_2O_2	MTBE, 1 h	(*S*)-**2b**: 95, 80
6	**1b**	**5d** (10)	CHP	Et_2O, 45 min.	(*S*)-**2b**: 99, 93
7	**1b**	**5d** (1)	CHP	Et_2O, 24 h	*no reaction*
8*	**1b**	**5d** (1)	CHP	K_2CO_3 (1 equiv), Et_2O, 10 h	(*S*)-**2b**: 98, 93
9	**1b**	**5d** (0.5)	CHP	K_2CO_3 (1 equiv), Et_2O, 48 h	(*S*)-**2b**: 98, 93
10†‡	**3b**	**5a** (0.05)	CHP	K_2CO_3 (1 equiv), Et_2O, 24 h	(*R*)-**4b**: 99, 88

* 1.5 g-scale. † 1 g-scale. ‡ No reaction occurred in the absence of K_2CO_3.

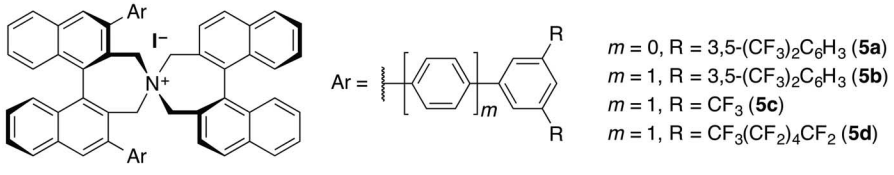

Fig. 2. Investigation of six-membered ring oxidative cyclization. (**A**) Comparison of five- and six-membered enantioselective oxidative cyclizations. Isolated yields of **2a**, **4a**, and **6** are reported. TBS, *tert*-butyldimethylsilyl. (**B**) Proposed catalytic mechanism and side-reaction pathway. "X" (in XOOH), H or alkyl. (**C**) Investigation of reaction parameters toward α-tocopherol. Isolated yields of **2b** and **4b** are reported. ee was determined by means of chiral stationary-phase high-performance liquid chromatography (HPLC). The absolute configuration of **2b** was determined by comparing the optical rotation of **9** (Fig. 3B) derived from **2b** with the literature value (*31*), and all other chromans **2** were assigned through analogy. The absolute configurations of **4a** and **4b** were determined by using their known analogs (*20*).

To prevent undesired dearomatization and accelerate the desired cyclization path, a *para*-toluenesulfonyl (Ts) group was introduced as an electron-withdrawing protective group in place of the silyl group of **1a**. As expected, the oxidative cyclization of **1b** with 10 mol % of (*R*,*R*)-**5a** gave desired (*R*)-**2b** quantitatively, with 60% ee (Fig. 2C, entry 1). The 3,3′-substituents of the binaphthyl moiety of (*R*,*R*)-**5** had a dramatic

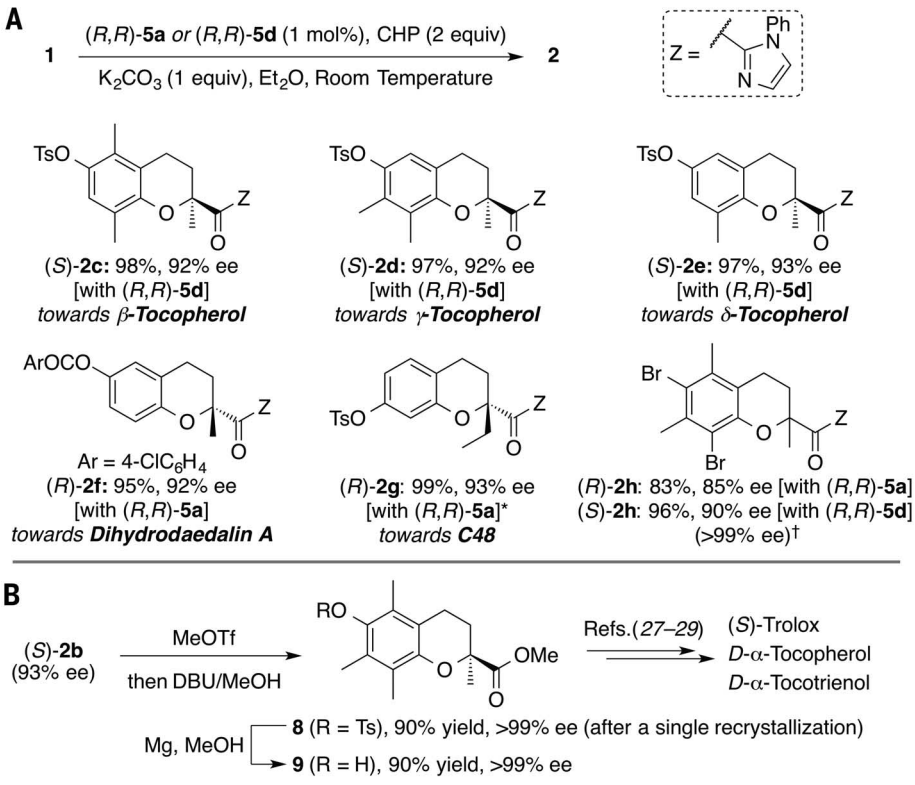

Fig. 3. Application to structurally diverse substrates. (**A**) Enantioselective oxidative cycloetherification of various γ-(2-hydroxyphenyl)ketones **1** to chromans **2**. Unless otherwise noted, 1 mol % of (*R*,*R*)-**5a** or (*R*,*R*)-**5d** was used in the presence of potassium carbonate. Asterisk indicates that the reaction was performed by using 10 mol % (*R*,*R*)-**5a** in the absence of K_2CO_3 with TBHP instead of CHP at 0°C. Dagger symbol indicates that (*R*)-**2h** and (*S*)-**2h** were obtained in optically pure forms after a single re-crystallization. (**B**) Asymmetric formal syntheses of (*S*)-trolox, *D*-α-tocopherol, and *D*-α-tocotrienol. MeOTf, methyl trifluoromethanesulfonate; DBU, 1,8-diazobicyclo[5.4.0]undec-7-ene.

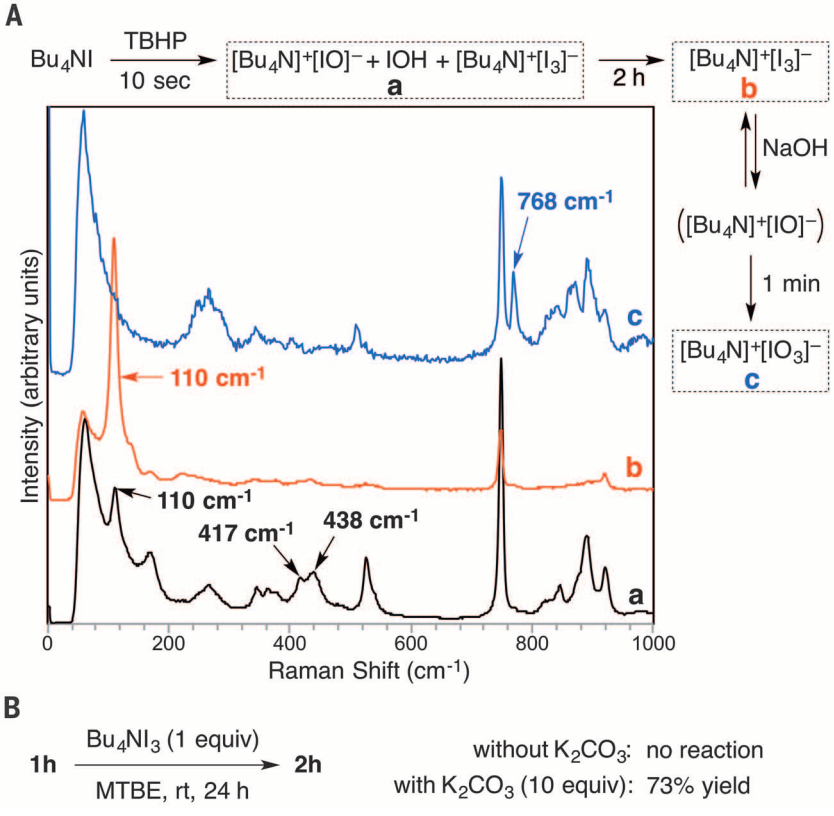

Fig. 4. Probing the active catalyst. (**A**) Detection of catalytic species. A series of Raman spectra (**a** to **c**) obtained upon the addition of sodium hydroxide to a solution of *n*-tetrabutylammonium iodide and TBHP are shown. (**B**) Control experiments with *n*-tetrabutylammonium triiodide in the presence or absence of potassium carbonate.

effect on enantioselectivity and reactivity (Fig. 2C, entries 1 to 4). To our surprise, the use of (*R*,*R*)-**5b** in place of (*R*,*R*)-**5a** gave (*S*)-**2b** as an opposite enantiomer, with higher enantioselectivity (86% ee) (Fig. 2C, entry 2). The opposite absolute stereoselectivity was observed with the use of not only (*R*,*R*)-**5b** but also (*R*,*R*)-**5c** and (*R*,*R*)-**5d**, which have biphenyl groups at the 3,3′ positions (Fig. 2C, entries 2 to 4). The best result (96% yield, 89% ee) was obtained after a shorter reaction time with perfluoroalkyl-substituted ammonium iodide (*R*,*R*)-**5d** (Fig. 2C, entry 4). Because the oxidative cyclization step might not be rate-limiting for **1b**, which was more reactive than **1a**, hydrogen peroxide could be used as an oxidant, albeit with a slightly reduced enantioselectivity (Fig. 2C, entry 5). When cumene hydroperoxide (CHP) was used as an oxidant in diethyl ether, the reaction was complete in 45 min, and (*S*)-**2b** was obtained quantitatively, with 93% ee (Fig. 2C, entry 6).

A reduction in the catalyst loading might cause competition between inactivation (path **c**) and oxidative cyclization (path **b**) in this catalytic system (Fig. 2B). When 1 mol % of **5d** was used, no reaction occurred, and the starting material was recovered fully (Fig. 2C, entry 7). To overcome this problem, suppression or reversible control of the inactivation path was considered. It is known that hypoiodite salts can be prepared with the hydrolysis of triiodide salts in alkaline solutions, and these species are in equilibrium under basic conditions (*26*). We envisioned that the hypoiodite species might be regenerated from triiodide species in the presence of appropriate base additives under our catalytic conditions. After the investigation of various organic and inorganic base additives (table S4), we succeeded in developing a high-performance catalytic oxidation system in the presence of an inorganic base such as potassium carbonate. Thus, the catalyst loading could be reduced to 1 or even 0.5 mol % [turnover number (TON) of the catalyst = 200] for the oxidation of **1b** in the presence of one equivalent of potassium carbonate without reducing the chemical yield or enantioselectivity (Fig. 2C, entries 8 and 9). Furthermore, the TON of the catalyst was 2000 for the five-membered oxidative cyclization of **3b** (Fig. 2C, entry 10). These reaction conditions were compatible with gram-scale synthesis (Fig. 2C, entries 8 and 10).

We examined several γ-(2-hydroxyphenyl) ketones **1** under optimized conditions (Fig. 3A). (*S*)-2-Acylchromans **2c**–**e**, which would be a synthetic intermediate for β-, γ-, and δ-tocopherols, were obtained quantitatively with high enantioselectivities by using 1 mol % of (*R*,*R*)-**5d**. The reactions of γ-[5-(4-chlorobenzoyloxy)-2-hydroxyphenyl]ketone **1f** and γ-(4-tosyloxy-2-hydroxyphenyl)ketone **1g** by using (*R*,*R*)-**5a** gave (*R*)-**2f** and (*R*)-**2g**, respectively. Compounds (*R*)-**2f** and (*R*)-**2g** would potentially offer a different route to dihydrodaedalin A (*11*, *12*) and Merck's compound C48 (*13*), respectively. The oxidative cyclizations of **1h** by using 1 mol % of (*R*,*R*)-**5a** and (*R*,*R*)-**5d** under the same conditions provided both enantiomers of the chroman **2h** with high enantioselectivities. The optically pure enantiomers **2h** could be obtained after a single recrystallization.

The formal syntheses of *D*-α-tocopherol, *D*-α-tocotrienol, and (*S*)-trolox were also achieved (Fig. 3B). The (*N*-phenylimidazol-2-yl)carbonyl group of product **2b** was easily transformed (*23*) to the methyl ester (**8**), which could be obtained in optically pure form after a single recrystallization. Subsequent deprotection of the tosyl group of **8** under mild conditions gave **9** in high chemical yield. The ester **9** is a common synthetic intermediate for *D*-α-tocopherol (*27*), *D*-α-tocotrienol (*28*), and (*S*)-trolox (*29*). Other tocopherols and their biologically active analogs could be easily prepared in a similar manner.

To gain insight into the catalytic mechanism, we performed various control experiments and spectroscopic analysis (Fig. 4, tables S5 and S6, and figs. S1 to S8). A series of Raman spectra obtained upon the addition of sodium hydroxide to a solution of *n*-tetrabutylammonium iodide (Bu_4NI) and TBHP is shown in Fig. 4A. To our delight, we detected unstable hypoiodite $[IO]^-$ and hypoiodous acid [IOH] species (*30*). Spectrum **a**, which includes three main bands at 110, 417, and 438 cm^{-1}, was recorded immediately after the mixing of Bu_4NI with TBHP. The other bands were attributed to the solvents and reagents used. The band at 110 cm^{-1} is characteristic of $[I_3]^-$. The bands at 417 and 438 cm^{-1} were assigned to $[IO]^-$ and [IOH] species, respectively, on the basis of the literature (*30*) and our control experiments (figs. S4 to S7). These two species might be in equilibrium under these conditions and disappeared steadily with time, and only a band of triiodide was observed after 2 hours (spectrum **b**). No other inert species such as iodate and periodate were observed at this time. The band of triiodide decreased immediately under basic conditions (spectrum **c**). A new band at 768 cm^{-1}, which is characteristic of the iodate $[IO_3]^-$ spectrum, was observed (*30*). This indicated the rapid generation and subsequent disproportionation of hypoiodite species (*30*). These results revealed that hypoiodite is an unstable catalytic active species and that triiodide is a stable inert species under our conditions (Fig. 2B). Although iodite species $[IO_2]^-$ could not be detected, we could not completely rule out a catalytic role of $[IO_2]^-$. The regeneration of hypoiodite from triiodide was also confirmed with control experiments (Fig. 4B and table S6). Oxidative cyclization of **1h** did not occur with the use of *n*-tetrabutylammonium triiodide but proceeded in the presence of potassium carbonate under identical conditions.

REFERENCES AND NOTES

1. H. C. Shen, *Tetrahedron* **65**, 3931–3952 (2009) and references therein.
2. T. Netscher, *Vitam. Horm.* **76**, 155–202 (2007) and references therein.
3. J. E. Packer, T. F. Slater, R. L. Willson, *Nature* **278**, 737–738 (1979).
4. The Alpha-Tocopherol Beta Carotene Cancer Prevention Study Group, *N. Engl. J. Med.* **330**, 1029–1035 (1994).
5. D. H. Blatt, W. A. Pryor, J. E. Mata, R. Rodriguez-Proteau, *J. Nutr. Biochem.* **15**, 380–395 (2004).
6. M. Tomasetti, J. Neuzil, *Vitam. Horm.* **76**, 463–491 (2007).
7. A. C. Howard, A. K. McNeil, P. L. McNeil, *Nat. Commun.* **2**, 597 (2011).
8. P.-H. Huang *et al.*, *Sci. Signal.* **6**, ra19 (2013).
9. W. Walther, W. Vetter, T. Netscher, *J. Micro. Sep.* **4**, 45–49 (1992).
10. G. V. López *et al.*, *Bioorg. Med. Chem.* **13**, 5787–5796 (2005).
11. M. Sekimoto, Y. Hattori, K. Morimura, M. Hirota, H. Makabe, *Bioorg. Med. Chem. Lett.* **20**, 1063–1064 (2010).
12. Y. Morimura, M. Hirota, Y. Hattori, H. Makabe, "Chroman compound and method for preparing the same," Japan patent 5212969 (2013).
13. H. Koyama *et al.*, *J. Med. Chem.* **47**, 3255–3263 (2004).
14. B. M. Trost, H. C. Shen, L. Dong, J.-P. Surivet, C. Sylvain, *J. Am. Chem. Soc.* **126**, 11966–11983 (2004).
15. L. F. Tietze, K. M. Sommer, J. Zinngrebe, F. Stecker, *Angew. Chem. Int. Ed. Engl.* **44**, 257–259 (2004).
16. S. Tanaka, T. Seki, M. Kitamura, *Angew. Chem. Int. Ed. Engl.* **48**, 8948–8951 (2009).
17. A. Chougnet, K. Liu, W.-D. Woggon, *Chimia (Aarau)* **64**, 303–308 (2010) and references therein.
18. S. Tokunou, W. Nakanishi, N. Kagawa, T. Kumamoto, T. Ishikawa, *Heterocycles* **84**, 1045–1056 (2012).
19. B. List, K. Maruoka, Eds., *Science of Synthesis: Asymmetric Organocatalysis* (George Thieme Verlag, Stuttgart, 2012).
20. M. Uyanik, H. Okamoto, T. Yasui, K. Ishihara, *Science* **328**, 1376–1379 (2010).
21. M. Uyanik, K. Ishihara, *ChemCatChem* **4**, 177–185 (2012).
22. T. Ooi, K. Maruoka, *Angew. Chem. Int. Ed. Engl.* **46**, 4222–4266 (2007).
23. D. A. Evans, K. R. Fandrick, H.-J. Song, K. A. Scheidt, R. Xu, *J. Am. Chem. Soc.* **129**, 10029–10041 (2007).
24. D. Magdziak, S. J. Meek, T. R. R. Pettus, *Chem. Rev.* **104**, 1383–1430 (2004).
25. R. D. Cadle, H. Huff, *J. Phys. Colloid Chem.* **54**, 1191–1195 (1950).
26. Y.-T. Chia, thesis, University of California, Berkeley (1958).
27. M. Nozawa, K. Takahashi, K. Kato, H. Akita, *Chem. Pharm. Bull. (Tokyo)* **48**, 272–277 (2000).
28. R. Chênevert, G. Courchesne, N. Pelchat, *Bioorg. Med. Chem.* **14**, 5389–5396 (2006).
29. A. Ida, Y. Kyuko, T. Hidaka, "Method of producing (*S*)-(−)-6-hydroxy-2,3,7,8-tetramethylchromane-2-carboxylic acid and product obtained by the method," U.S. Patent 8,080,676 (2011).
30. J. C. Wren, J. Paquette, S. Sunder, B. L. Ford, *Can. J. Chem.* **64**, 2284–2296 (1986).
31. H. Yoda, K. Takabe, *Chem. Lett.* **18**, 465–466 (1989).

ACKNOWLEDGMENTS

Financial support for this project was partially provided by the Japan Society for the Promotion of Science, Grant-in-Aid for Scientific Research (KAKENHI) (24245020, 22750087, and 25105722), and Program for Leading Graduate Schools "Integrative Graduate Education and Research in Green Natural Sciences," Ministry of Education, Culture, Sports, Science and Technology, Japan. Metrical parameters for the structure of compound **2h** are available free of charge from the Cambridge Crystallographic Data Centre under reference number CCDC 996935. M.U. and K.I. developed the concept and conceived the experiments. H.H. performed the experiments. H.H. and M.U. analyzed the data. M.U. and K.I. prepared the manuscript, with assistance from H.H.

SUPPLEMENTARY MATERIALS

www.sciencemag.org/content/345/6194/291/suppl/DC1
Materials and Methods
Tables S1 to S7
Figs. S1 to S9
HPLC Traces
NMR Chart
References (*32*–*53*)

18 April 2014; accepted 10 June 2014
10.1126/science.1254976